

# ACTIVE BELITE $\beta$ -C<sub>2</sub>S AND THE HYDRATION OF CALCIUM SULFOALUMINATES PREPARED FROM NANO-MATERIALS

H. EL- DIDAMONY\*, #MOHAMED HEIKAL\*\*, \*\*\*, T.M.EL-SOKKARY\*\*\*\*, KH. A. KHALIL\*, I.A. AHMED\*\*\*\*\*

\*Chemistry Department, Faculty of Science, Zagazig University, Zagazig, Egypt

\*\*Chemistry Department, College of Science, Al Imam Mohammad Ibn Saud, Islamic University (IMSIU),  
P.O Box 90950, Riyadh 11623, Saudi Arabia

\*\*\*Chemistry Department, Faculty of Science, Benha University, Benha, Egypt

\*\*\*\*Housing and Building Research Centre Cairo, Egypt

\*\*\*\*\*Chemistry Department, Faculty of Science and Art, King Kalid University, KSA

#E-mail: ayaheikal@hotmail.com

Submitted April 9, 2014; accepted July 25, 2014

**Keywords:** Calcium sulfoaluminate C<sub>4</sub>A<sub>3</sub>S̄, Belite  $\beta$ -C<sub>2</sub>S, Hydration Products, Thermal Analysis, X-Ray Diffraction

*The aim of the present work is to study the effect of active belite on the hydration of C<sub>4</sub>A<sub>3</sub>S̄ and C<sub>4</sub>A<sub>3</sub>S̄. The results revealed that the active  $\beta$ -C<sub>2</sub>S prevents the formation of crystalline ettringite and monosulfate hydrate as detected from the results of XRD. On the other side, the sulfoaluminate hydrates such as AFt and AFm were detected by using DSC technique. Gismondine C<sub>4</sub>Al<sub>8</sub>Si<sub>8</sub>O<sub>32</sub>·16H is formed from the reaction of  $\beta$ -C<sub>2</sub>S or CSH with the liberated Al(OH)<sub>3</sub> from the hydration of C<sub>4</sub>A<sub>3</sub>S̄. This phase was not detected with the other monosulfate mix C<sub>4</sub>A<sub>3</sub>S̄. This is mainly due to the absence of AH<sub>3</sub> during the hydration of C<sub>4</sub>A<sub>3</sub>S̄. The results of XRD patterns are in good agreement with those obtained from DSC thermograms.*

## INTRODUCTION

The productions of specific cements based on C<sub>4</sub>A<sub>3</sub>S̄ have been making great progress [1]. Researchers found that nano-particles dispersed in a cement paste will accelerate cement hydration due to their high activity. Additionally, nano-particles will fill the open pore systems to increase strength as well as improve the microstructure of cement and the interface between the cement paste and aggregates in concrete [2]. The hydration mechanisms of two sulfoaluminate cements by experimental means of thermodynamic modeling were explained. Upon hydration of yeelimite C<sub>4</sub>A<sub>3</sub>S̄ during the first hours, ettringite and AH<sub>3</sub> are formed. If belite phase is present as a minor phase, gehlenite-like hydrate forms as a further hydration product consuming a part of the amorphous AH<sub>3</sub>. The formation of C-S-H phase was not observed [3]. The silica dissolved and incorporated into strätlingite (C<sub>2</sub>ASH<sub>8</sub>) which is oversaturated throughout the hydration period. It was concluded that in calcium sulfoaluminate belite cements as the C<sub>4</sub>A<sub>3</sub>S̄ content increases, the amounts of ettringite and amorphous AH<sub>3</sub> increase [4]. The large source of ettringite and AH<sub>3</sub> increases the sensitivity of the cement to other factors that cause expansion.

Belite and sulfobelite cements might reduce the impact on the environment and global warming, caused by the production of ordinary Portland cement (OPC) [5-7]. The lower required amount of carbonates and the reduction of CO<sub>2</sub> emission, due to the lower firing temperature when compared to OPC clinker, are important advantages of those alternative formulations [8]. In addition, the sulfobelite cement has its mineralogy based on calcium sulfoaluminate (C<sub>4</sub>A<sub>3</sub>S̄), belite ( $\beta$ -C<sub>2</sub>S), ferrite and calcium sulfate (CS̄). In general, it exhibits faster strength gain than belite-based cements, due to the presence of C<sub>4</sub>A<sub>3</sub>S̄. Belite is the main phase responsible for hardening at later ages.

Martin-Sedeno *et al.*, [9] investigated the hydration processes of three aluminum-rich belite sulfoaluminate cements. Živica [10] evaluated blends of sulphaluminate belite containing distinct pozzolans (blastfurnace slag, fly ash, and silica fume) in terms of setting time and compressive strength development. Mortars prepared with ettringite-rich sulfoaluminate cements exhibit faster hydration and higher self-desiccation than those containing OPC [11]. It was found that mortars prepared from blends of sulfoaluminate belite-OPC exhibited higher protection against corrosion of steel in comparison to those of blastfurnace slag -OPC binders [12].

In addition, the concrete made with sulfobelite exhibits early strength development and excellent sulfate resistance, but worse workability and higher carbonation rates than OPC based formulations [13].

The main minerals of calcium sulfoaluminate (CSA) cement are yeelimite ( $C_4A_3\bar{S}$ ), belite ( $\beta\text{-C}_2\text{S}$ ), gypsum ( $C\bar{S}H_2$ ) and the minor phases are calcium aluminate, tricalcium aluminate, ferrite, or gehlenite [14-17]. The main hydration products of CSA cement are ettringite (AFt) and monosulfate (AFm) as well as C-S-H phase,  $Al_2O_3$  and  $Fe_2O_3$  (aq.) [2].

The data provided in the literature on the hydration of ternary binders based on OPC, CSA clinker and calcium sulfate with similar binders based on laboratory synthesized materials are rare [18-20]. Therefore, the effect of active belite on the hydration mechanisms of  $C_4A_3\bar{S}\text{-CaSO}_4$  was studied.

The aim of the present work is to study the effect of active belite on the hydration of calcium sulfoaluminate ( $C_4A_3\bar{S}$ ) and monosulfate mix ( $C_4A\bar{S}$ ) using XRD and DSC techniques to show the main characteristics of hydration products up to 28 days. Also, the rate of reaction was also followed by the determination of chemically combined water contents, at different ages of hydration.

### EXPERIMENTAL

The materials used in this work were nano-Ca ( $NO_3$ )<sub>2</sub>, nano-Al(OH)<sub>3</sub>, nano-silica and  $CaSO_4 \cdot 2H_2O$  as obtained from Prolabo Company. Nano-Al(OH)<sub>3</sub> was prepared from Al-dross after leaching with commercial HCl then precipitated by ammonia solution at pH = 8 [21, 22]. Nano silica was also synthesized by acid hydrolysis of sodium silicate  $Na_2SiO_3$  using 0.5 N HCl and stirred slowly at 60°C at pH between 1 and 2 [23]. Nano-Ca( $NO_3$ )<sub>2</sub> was freshly prepared by the addition of nitric acid (1:1) to  $CaCO_3$  to complete reaction then evaporated at 60°C until solidification. The powder of  $Ca(NO_3)_2$  was dried at 50°C for 24 hrs. The materials were investigated for their chemical composition by using XRF, XRD and TEM. Table 1 summarizes the chemical composition of nano-SiO<sub>2</sub> and nano-Al(OH)<sub>3</sub>.

Figures 1 and 2 shows TEM micrograph of nano-SiO<sub>2</sub> and nano-Al(OH)<sub>3</sub>. Synthetic procedure and characterization of  $\beta\text{-C}_2\text{S}$  and calcium sulfoaluminate were reported [21]. The chemical oxide composition of  $C_4A_3\bar{S}$ ,  $C_4A\bar{S}$  and  $\beta\text{-C}_2\text{S}$  was given in Table 2.

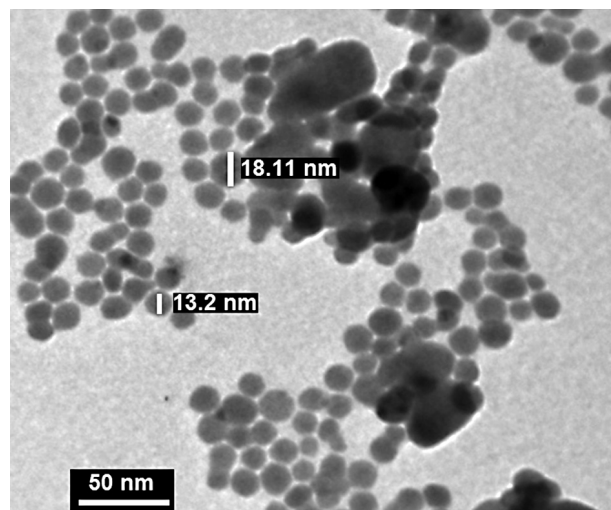


Figure 1. TEM micrograph of nano-SiO<sub>2</sub>.

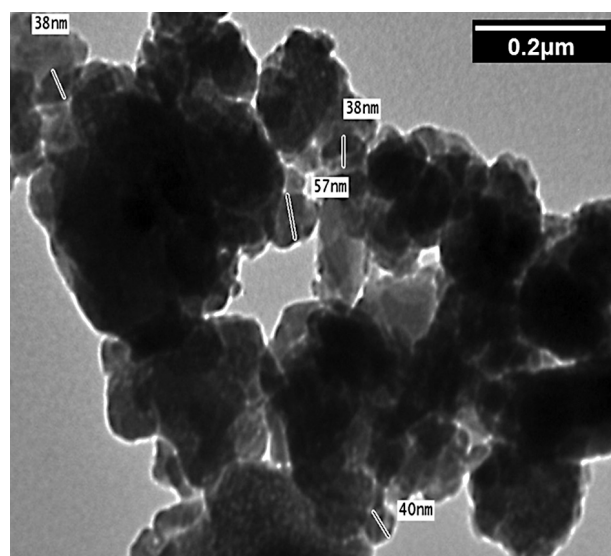


Figure 2. TEM micrograph of nano-Al(OH)<sub>3</sub>.

Table 1. Chemical oxide composition of synthesized materials (mass %).

Material	SiO <sub>2</sub>	Al <sub>2</sub> O <sub>3</sub>	Fe <sub>2</sub> O <sub>3</sub>	CaO	MgO	SO <sub>3</sub>	Na <sub>2</sub> O	K <sub>2</sub> O	L.O.I
Nano-SiO <sub>2</sub>	87.59	0.52	0.09	0.53	0.13	0.02	1.44	0.08	9.60
Nano-Al(OH) <sub>3</sub>	1.34	56.73	1.98	0.89	0.06	2.31	0.07	0.03	36.40

Table 2. Chemical oxide composition of the fired materials (mass %).

Materials	SiO <sub>2</sub>	Al <sub>2</sub> O <sub>3</sub>	Fe <sub>2</sub> O <sub>3</sub>	CaO	MgO	SO <sub>3</sub>	Na <sub>2</sub> O	L.O.I
$C_4A_3\bar{S}$	2.73	34.27	1.18	47.95	0.20	11.5	0.22	1.50
$C_4A\bar{S}$	1.60	22.12	0.40	54.02	0.20	17.5	0.31	4.05
$\beta\text{-C}_2\text{S}$	34.70	0.45	0.07	62.70	0.32	–	0.68	1.92

Different mixes from  $C_4A_3\bar{S}$  (SA) as well as  $C_4A\bar{S}$  (MS) were prepared and separately mixed with equal amounts of active belite (B). The investigated batches were  $C_4A_3\bar{S} + \beta$ - $C_2S$  (SAB) and  $C_4A\bar{S} + \beta$ - $C_2S$  (MSB) mixed with the suitable amount of normal water of consistency and pelletized [24], then cured in 100 % relative humidity till the time of testing. The hydration process was stopped as described in earlier publications [25]. The hydration kinetics of the investigated pastes were identified by the aid of XRD and DSC techniques as well as the determination of chemically combined water contents after firing at 1000°C for one hour, as the loss on ignited weight basis, as a function of curing time up to 72 hours.

## RESULTS AND DISCUSSION

### Hydration of $C_4A_3\bar{S}$ in the presence of $\beta$ - $C_2S$

#### X-ray diffraction analysis

Figure 3 illustrates the XRD diffractograms of hydrated  $C_4A_3\bar{S} + \beta$ - $C_2S$  (SAB) paste hydrated up to 7 days. The sample hydrated for 6 hrs shows the peaks characteristic for the anhydrous phases ( $C_4A_3\bar{S}$  and  $\beta$ - $C_2S$ ) with the appearance of portlandite from the hydration of active  $\beta$ - $C_2S$ . As hydration proceeds up to 24 hrs, the intensity of the peaks of  $C_4A_3\bar{S}$  is markedly decreased whereas those of belite phase are almost the same. After

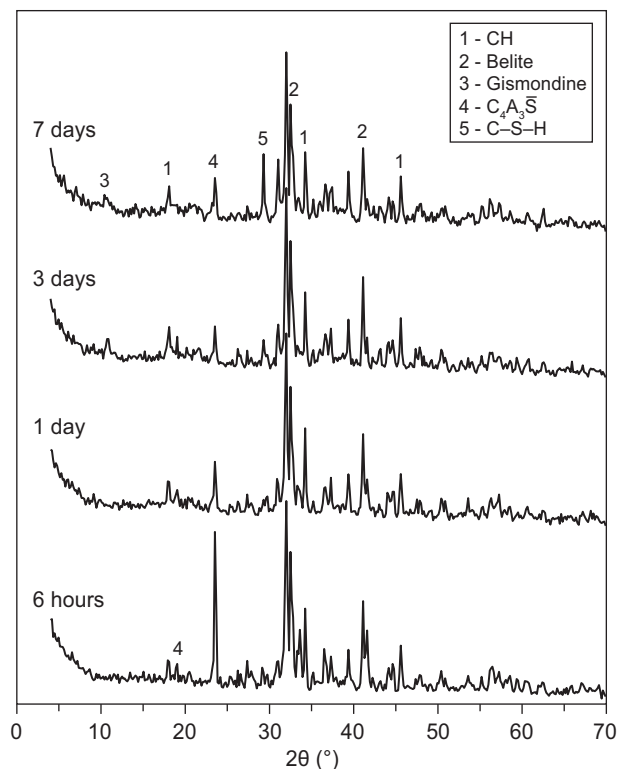


Figure 3. XRD diffractograms of  $C_4A_3\bar{S} + \beta$ - $C_2S$  - 3 days paste hydrated up to 7 days.

3 days of hydration, the calcium sulfoaluminate peaks decrease with the appearance of a new phase, namely, calcium aluminosilicate hydrate (Gismondine) with the formula  $(C_4Al_8Si_8O_{32} \cdot 16H)$  [26]. It was formed after 3 days and still with the same intensity with the presence of the residual anhydrous parts of  $C_4A_3\bar{S}$  phase at 7 days of hydration. Evidently, the high reactivity of belite or C-S-H, as a source of silica, can react with amorphous  $AH_3$  and portlandite with the formation of this phase. It can be concluded that the presence of active belite prevents the formation of crystalline sulfoaluminate hydrates such as ettringite (AFt) and monosulfate hydrate (AFm). The ettringite phase is not detected by XRD suggesting that ettringite was formed as very fine crystals [27]. The intensity of belite is slightly decreased after 7 days. During the hydration of belite, C-S-H is formed after one day and increases up to 7 days. On the other side, the hydration of neat  $C_4A_3\bar{S}$  in absence of  $\beta$ - $C_2S$  gives excess AFt with low content of AFm with residual  $C_4A_3\bar{S}$  [28].

Figure 4 shows the variation of the hydration products of pure  $C_4A_3\bar{S}$  and  $C_4A_3\bar{S}$ - $\beta$ - $C_2S$  mix after 3 days of hydration. From the X-ray diffractograms it is clear that the hydration of pure  $C_4A_3\bar{S}$  shows the formation of AFt with small amount of AFm in addition to the residual parts of unreacted phase ( $C_4A_3\bar{S}$ ). On the other side the presence of active belite with  $C_4A_3\bar{S}$  prevents the formation of any crystalline calcium sulfoaluminate hydrates (AFt or AFm) but leads to the formation calcium aluminosilicate hydrates, namely, gismondine ( $C_4Al_8Si_8O_{32} \cdot 16H$ ). This is due to the reaction of C-S-H with calcium aluminate hydrates or  $AH_3$  [2, 26].

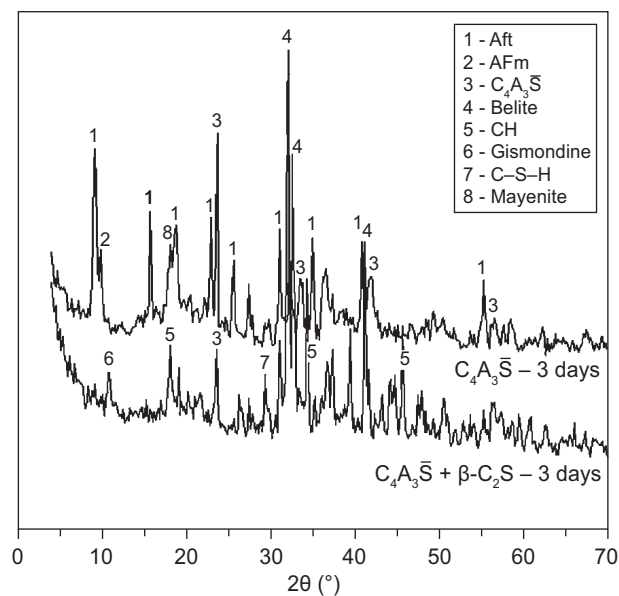


Figure 4. XRD diffractograms of  $C_4A_3\bar{S} + \beta$ - $C_2S$  paste in comparison with the neat  $C_4A_3\bar{S}$  paste hydrated after 3 days of hydration.

*Thermal analysis*

Figure 5 illustrates DSC thermograms of hydrated  $C_4A_3\bar{S}$  in the presence of active belite up to 28 days of hydration. The thermograms show five endothermic peaks located at 70, 130, 180, 270, 450°C, in addition to the endotherm at 725°C. The first endotherm located at 70°C may be due to the dehydration of ill-crystalline C-S-H. The endothermic effects at 130 and 180°C are related to the dehydration of ettringite (AFt) and monosulfate hydrate (AFm), respectively [26, 29, 30]. The intensities of the peaks increase with curing time up to 3 days of hydration due to the continuous hydration of  $C_4A_3\bar{S}$  [14, 16, 31]. The endotherm located at 270°C may be due to the decomposition of  $AH_3$ . This peak increases from 6 hours up to one day and then decreases up to 28 days. It is clear that the peak of  $AH_3$  decreases with curing time due to its reaction with C-S-H or  $\beta-C_2S$  to form gismondine which increases with time. There is a small broad endothermic peak at 450°C related to the hydroxylation of portlandite liberated during the hydration of belite. On prolong hydration the endothermic peak 220°C increases from 6 hours up to 28 days. The endothermic peak located at 725°C is mainly due to the decomposition of  $CaCO_3$ . Martine-Sedeno et al. [9] investigated the early hydration of aluminum-rich belite sulfoaluminate cements.  $\beta-C_2S$  reacts at early ages (3 hrs) compared to belite-rich Portland cement in which this phase does not react during the first month. The early hydration of  $\beta-C_2S$  in these belite- sulfoaluminate

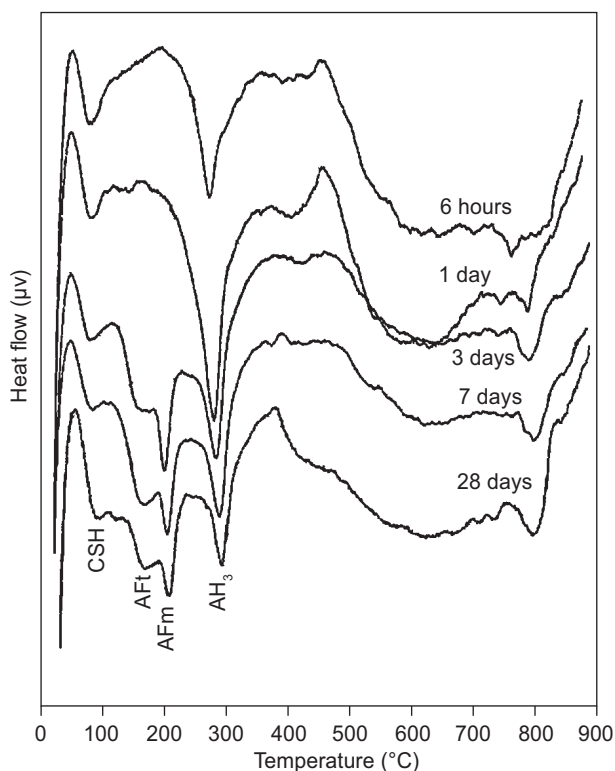


Figure 5. DSC thermograms of the hydrated  $C_4A_3\bar{S}$  +  $\beta-C_2S$  paste up to 28 days of hydration.

cements is not the usual reaction to yield C-S-H gel and portlandite, as portlandite is not detected in these pastes. Instead, belite appears to react with amorphous  $AH_3$  to yield gismondine; it was formed in this investigation as a hydrated calcium aluminosilicate hydrate.

Figure 6 shows the variation of hydration products of  $C_4A_3\bar{S}$  and belite at 3 days of hydration. The calcium sulfoaluminate, ( $C_4A_3\bar{S}$ ) gives ettringite as the main hydration product in addition to monosulfate hydrate and liberated  $AH_3$ . The presence of  $AH_3$  is due to the lack of anhydrite to give ettringite and/or monosulfate hydrate [28].

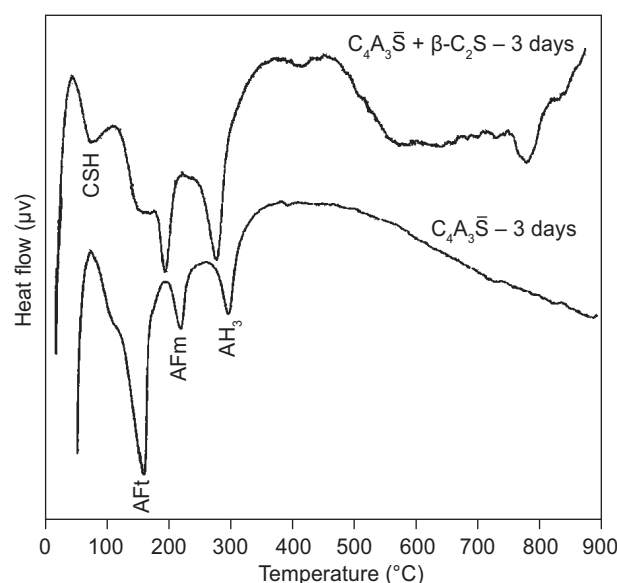


Figure 6. DSC thermograms of  $C_4A_3\bar{S}$  +  $\beta-C_2S$  paste hydrated at 3 days in comparison with the neat  $C_4A_3\bar{S}$  mix.

On the other side, the DSC of  $C_4A_3\bar{S}$  in the presence of  $\beta-C_2S$  hydrated up to 3 days shows the formation of C-S-H at nearly 100°C, instead of ettringite. The thermograms show also four other endothermic effects at 180, 280, 440 and 740°C. The second and third endothermic peaks are due to the decomposition of ettringite AFt and gismondine. The fourth peak located at 300°C may be due to the decomposition of residual  $AH_3$ . The endothermic peak at 740°C is attributed to the decomposition of  $CaCO_3$  due to the carbonation of  $Ca(OH)_2$ . It can be also said that this peak is related to the decomposition of the carbonated C-S-H. The  $CaCO_3$  is not formed in the hydration of pure  $C_4A_3\bar{S}$  due to the absence of portlandite in the hydration of this phase.  $\beta-C_2S$  liberates portlandite which can be carbonated.

Hydration of  $C_4A\bar{S}$  Mix with Active  $\beta-C_2S$

*X-ray diffraction analysis*

X-ray diffractograms obtained for the paste made of 50 %  $C_4A\bar{S}$  - 50 %  $\beta-C_2S$  mix, (by weight) compared

with the neat  $C_4A\bar{S}$  mix as seen in Figure 7 at different ages of hydration. From XRD diffractograms, ettringite or monosulphate phases are not detected. This may be due to the poorly crystalline phases. The alkalinity of the hydration environment deriving from the hydration of belite phase ( $\beta$ - $C_2S$ ) tends to increase alkali content [32]. The formed ettringite from the hydration of  $C_4A_3\bar{S}$  in this medium is very fine crystals; therefore it is not detected by the XRD analysis. Sample hydrated for 6 hrs illustrates the presence of the anhydrous phases such as belite ( $\beta$ - $C_2S$ ) anhydrite in addition to portlandite. As the hydration proceeds up to one day, the peaks of  $C_4A_3\bar{S}$ , anhydrite, portlandite and belite decrease. The sample hydrated for 3 days shows the appearance of C-S-H which is overlapped by the  $CaCO_3$  and increases up to 7 days. At 7 days, the intensity of  $C_4A\bar{S}$  sharply decreases with the disappearance of anhydrite  $CaSO_4$  and the presence of belite phase. This means that the formation of hydrated calcium sulfoaluminate hydrates such as Aft or AFm are amorphous, i.e. the ettringite or monosulphate hydrate cannot be formed as crystalline phases in the presence of active belite as shown in the hydration of pure  $C_4A\bar{S}$ .

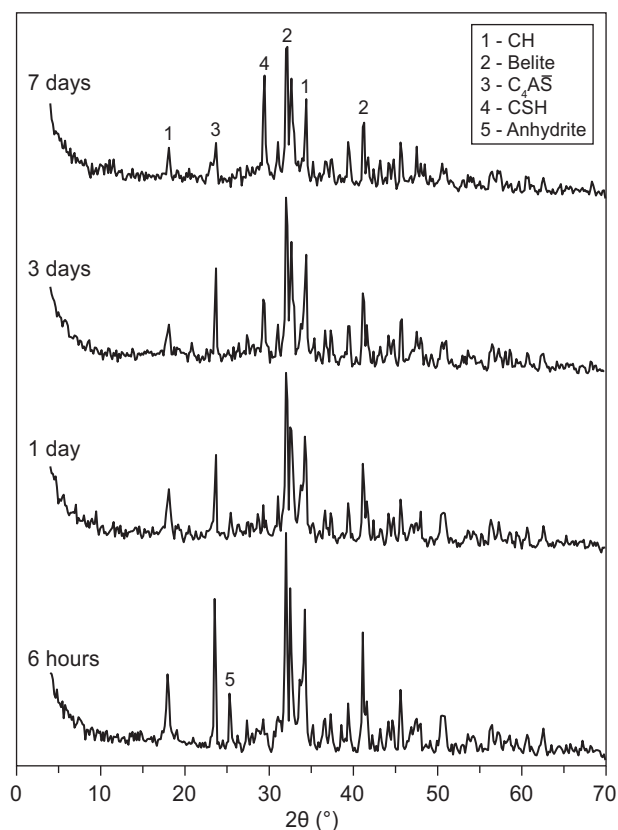


Figure 7. XRD diffractograms of  $C_4A_3\bar{S} + \beta$ - $C_2S$  paste hydrated up to 7 days.

Figure 8 illustrates the variation of the hydration products of pure monosulphate mix  $C_4A\bar{S}$  in comparison with equal amounts of  $C_4A\bar{S} + \beta$ - $C_2S$  hydrated at 3 days.

The neat sulfoaluminate mix shows the formation of well crystalline Aft as well as AFm with residual  $C_4A\bar{S}$  and portlandite with the disappearance of  $CaSO_4$ . On the other side, the presence of belite with  $C_4A\bar{S}$  prevents the formation of any crystalline sulfoaluminate phases such as Aft or AFm. The calcium sulfoaluminate phase  $C_4A\bar{S}$  is still presents as residual phase with the appearance of C-S-H with  $CC$  and some portlandite. The anhydrite peak is completely disappeared.

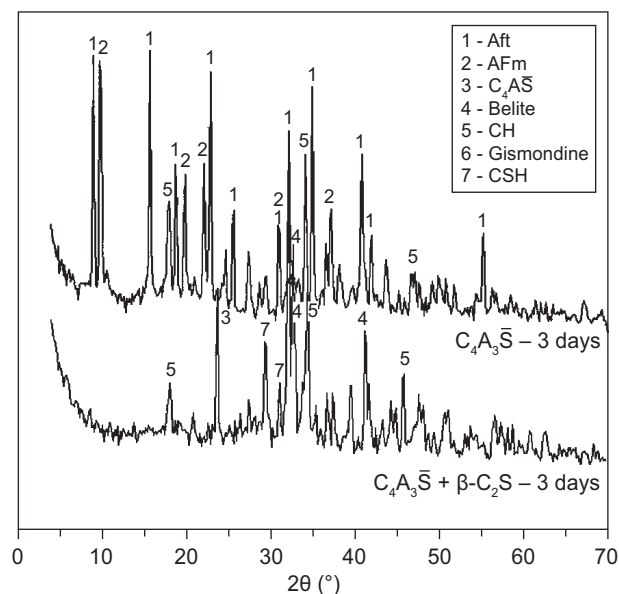


Figure 8. XRD diffractograms of  $C_4A\bar{S} + \beta$ - $C_2S$  paste in comparison with the neat  $C_4A\bar{S}$  after 3 days of hydration.

#### Thermal analysis

The DSC thermograms of belite with monosulfate ( $C_4A\bar{S} + \beta$ - $C_2S$ ) mix hydrated for different curing times are shown in Figure 9. DSC thermogram of sample hydrated for 6 hours demonstrates the existence of three endothermic peaks at 80, 450, and 735°C. The endotherm at 80 is related to the lattice water of poorly crystalline C-S-H. The ettringite peak appeared at 130°C after 3 days of hydration indicating this low rate of hydration of  $C_4A\bar{S}$  up to 3 days which increases after 7 days.

The peak at 450°C represents the decomposition of portlandite which liberated during the hydration of belite. The peak of portlandite decreases with curing time due to the reaction with  $C_4A_3\bar{S}$  and anhydrite forming ettringite which is increased with curing time. The endothermic peak located at 735°C is related to the decomposition of  $CaCO_3$  due to the carbonation of some of portlandite that found in the fired monosulfate in addition to its liberation from belite.

The results of the DSC of monosulfoaluminate mix with active belite indicate that the monosulfate hydrate is not formed in comparison with pure  $C_4A\bar{S}$  mix

which gives after hydration ettringite and monosulfate hydrate. Belite inhibits the formation of ettringite in the monosulfate-belite mix.

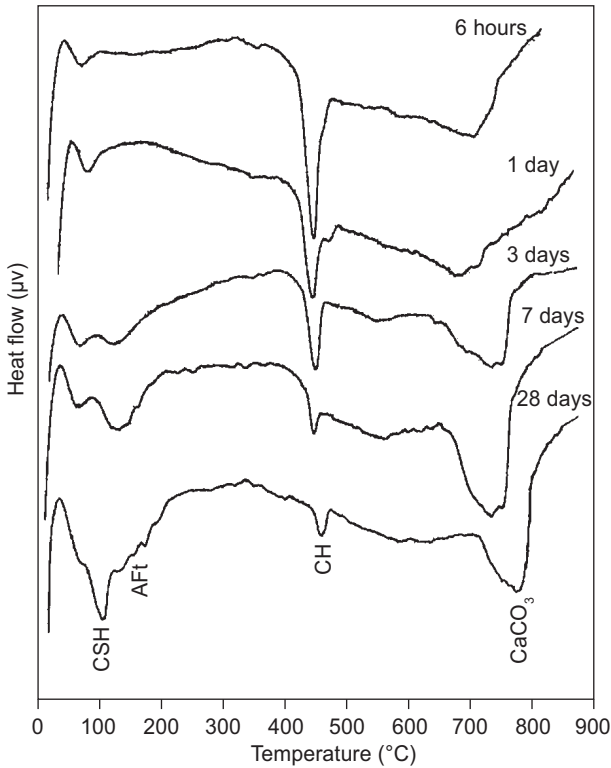


Figure 9. DSC thermograms of the hydrated  $C_4A_3\bar{S} + \beta-C_2S$  paste up to 28 days.

Figure 10 shows the effect of belite phase on the hydration of  $C_4A_3\bar{S}$  mix as shown from DSC thermograms hydrated at 3 days. It is clear that that the DSC thermogram of pure  $C_4A_3\bar{S}$  mix shows the formation of AFt, AFm and/or  $AH_3$  with the detection of some portlandite. The effect of belite on the hydration of that mix shows the endothermic peaks at 80, 130, 440, and  $\sim 750^\circ\text{C}$ . The first endothermic peak is due to the formation of C-S-H from the hydration of belite, in addition to the free lime in

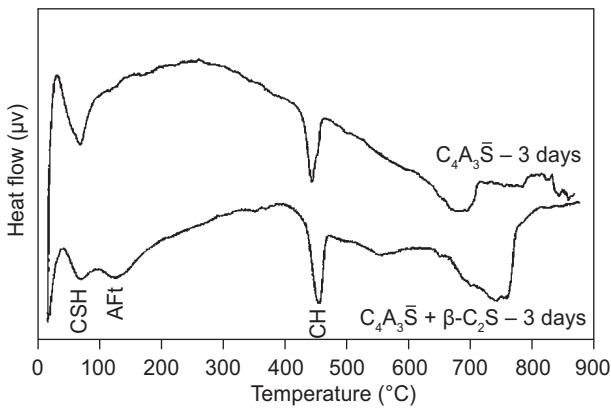


Figure 10. DSC thermograms of  $C_4A_3\bar{S} + \beta-C_2S$  paste hydrated at 3 days in comparison with the neat monosulphate mix.

the fired mix  $C_4A_3\bar{S}$ . It can be said that the belite prevents the formation of monosulfate hydrate. The portlandite decreases after 3 days of hydration due to stabilization of ettringite as a result of high pH provided or by its carbonation.

#### Combined water content

Figure 11 shows the chemically combined water contents of SAB and MSB pastes as a function of curing time up to 72 hours. The chemically combined water contents increase with the curing time due to the continuous hydration. Generally, MSB gives higher water contents than those of SAB pastes, this is due to the presence of free lime and anhydrite  $\text{CaSO}_4$  in the fired mix of monosulfate which can hydrate giving  $\text{Ca}(\text{OH})_2$  with the formation of ettringite as well as monosulfate hydrate. These phases have higher combined water contents in addition to the carbonation of some portlandite. The low water contents of SAB are mainly due to the absence of portlandite which can activate the SA to give ettringite and may be carbonated. This is seen from the endothermic peak of  $\text{CaCO}_3$  in SAB in comparison with MSB. The rate of hydration of each paste is slightly increased up to one day. This means that the sulfoaluminate phases are slightly hydrated at the early age of hydration up to one day in the presence of belite. On prolong hydration the rate of hydration of SAB and MSB pastes is sharply increased up to 72 hours. This is due to the continuous hydration of active belite forming C-S-H with  $\text{Ca}(\text{OH})_2$ . The combined water contents of pure sulfoaluminate pastes are lower than those of SAB and MSB. The SA and SAB give 32.65 and 38.55 % combined water contents upon hydration for 72 hours, respectively; whereas those of MS and MSB are 17.14 and 20.20 % [28]. This means that the belite increases the amount of combined water contents in the presence of calcium sulfoaluminates.

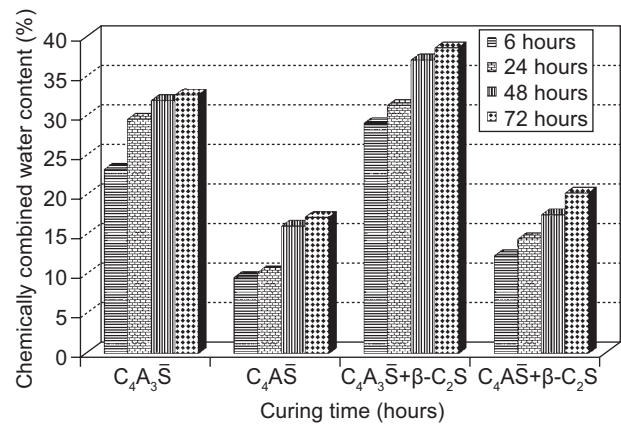


Figure 11. Chemically combined water contents of  $C_4A_3\bar{S} + \beta-C_2S$  and  $C_4A_3\bar{S} + \beta-C_2S$  pastes in comparison with neat  $C_4A_3\bar{S}$  and  $C_4A_3\bar{S}$  mixes as a function of curing time up to 72 hours.

## CONCLUSION

From the above results it can be concluded that:

The active  $\beta$ -C<sub>2</sub>S-C<sub>4</sub>A<sub>3</sub> $\bar{S}$  inhibits the formation of crystalline calcium sulphoaluminate hydrates (AFt or AFm) as revealed from the results of XRD and DSC. Calcium aluminosilicate hydrate (Gismondine, (C<sub>4</sub>Al<sub>8</sub>Si<sub>8</sub>O<sub>32</sub>·16H)) is formed from the reaction of  $\beta$ -C<sub>2</sub>S or C-S-H with the liberated AH<sub>3</sub> from hydrated C<sub>4</sub>A<sub>3</sub> $\bar{S}$ . On the other side, this phase is not formed with the hydration products of C<sub>4</sub>A $\bar{S}$ -belite mix due to the absence of AH<sub>3</sub> in this system. The chemically combined water contents of SA and MS pastes are lower than those of SAB and MSB pastes.

## Acknowledgment

*The authors would like to thank Prof. Dr. Mohamed Heikal, Professor of Inorganic Chemistry and Building materials, Chemistry Department, College of Science, Al Imam Mohammad Ibn Saud, Islamic University (IMSIU), P.O Box 90950, Riyadh 11623, Saudi Arabia, for his great help throughout the interpretation of the results of this article.*

## REFERENCES

1. Wu Z., Lu K.: J. Chin. Ceram. Soc. 20, 365 (1992).
2. Hui Li., Xiao H. G., Ou J. P.: Cem. Concr. Res. 34, 435 (2004).
3. Winnefeld F., Lothenbach B.: Cem. Concr. Res. 40, 1239 (2010).
4. Chen I.A., Hargis C.W., Juenger M. G: Cem. Concr. Res. 42, 51 (2012).
5. Senff L., Castela A., Hajjaji W., Hotza D., Labrincha J.A.: Const. Build. Mater. 25, 3410 (2011).
6. Popescu C.D., Muntean M., Sharp J.H.: Cem. Concr. Comp. 25, 689 (2003).
7. Chatterjee A.K.: Cem. Concr. Res. 26, 1213 (1996).
8. Hewlett P.C.: *Lea's chemistry of cement and concrete*, London, Arnold 2000.
9. Martín-Sedeño M.C., Cuberos A.J.M., De La Torre A.G., Álvarez-Pinazo G., Ordóñez L.M., Gatheshki M., Aranda M. A. G.: Cem. Concr. Res. 40, 359 (2010).
10. Živica V.: Const. Build. Mater. 14, 433 (2000).
11. Glasser F.P., Zhang L.: Cem. Concr. Res. 31, 1881 (2001).
12. Janotka I., Krajčí L., Ray A., Mojumdar S.C.: Cem. Concr. Res. 33, 489 (2003).
13. Quillin K.: Cem. Concr. Res. 31, 1341 (2001).
14. Liao Y., Wei X., Li G.: Const. Build. Mater. 25, 1572 (2011).
15. Péra J., Ambroise J.: Cem. Concr. Res. 34, 671 (2004).
16. Gastaldi D., Canonico F., Boccaleri E.: J. Mater. Sci. 44, 5788 (2009).
17. Lan W., Glasser F.P.: Adv. Cem. Res. 8, 127 (1996).
18. Pelletier L., Winnefeld F., Lothenbach B. in: 17<sup>th</sup> Inter. Baustofftagung (ibautil), p. 277-82, Weiwar, Germany, 2009.
19. Pelletier L., Winnefeld F., Lothenbach B.: Cem. Concr. Comp. 32, 497 (2010).
20. Taczuk I., Bayoux J.P., Sorrentino F., Capmas A. in: Proc. 9<sup>th</sup> ICCI, p.278-84, National Council for Cement and Building Materials, New Delhi, 1992.
21. El-Didamony H., Khalil Kh. A., Ahmed I.A., Heikal M.: Const. Build. Mater. 35, 77 (2012).
22. El-Didamony H., Khalil Kh.A., Heikal M.: Const. Build. Mater. 38, 14 (2013).
23. Mathew, Narayankutty S.K. in: International conference on advance in polymer technology, p. 279, India, 2010.
24. ASTM Designation: C- 191: *Standard test method for normal consistency and setting of hydraulic cement ASTM*, Annual Book cement of ASTM Standards, 2008.
25. El-Didamony H.: Thermchim. Acta. 35, 201 (1980).
26. Antiohos S., Papageorgiou A., Tsimas S.: Cem. Concr. Res. 36, 2123 (2006).
27. Haoxuan Li, Dinesh K. Agrawal, Jiping Cheng, Michael, Silsbee R.: Cem. Concr. Res. 31, 1257 (2001).
28. El-Didamony H., El-Sokkari T. M., Khalil Kh.A., Heikal M., Ahmed I.A.: Ceramics – Silikáty 56, 395 (2012).
29. Sherman N., Beretka J., Santoro L., Valenti G.L.: Cem. Concr. Res. 25, 113 (1995).
30. Pelletier L., Winnefeld F., Lothenbach B.: Cem. Concr. Comp. 32, 497 (2010).
31. Bernardo G., Telesca A., Valenti V.G.: Cem. Concr. Res. 36, 1042 (2006).
32. Kasselouri V., Tsakiridis P., Malami C, Georgali B., Alexandridou C.: Cem. Concr. Res. 25, 1726 (1995).